



## Research papers

# Past and future changes toward earlier timing of streamflow over Pakistan from bias-corrected regional climate projections (1962–2099)

Shahid Ali<sup>a</sup>, Byeong-Hee Kim<sup>a</sup>, Taimoor Akhtar<sup>c</sup>, Jonghun Kam<sup>a,b,\*</sup>

<sup>a</sup> Division of Environmental Science and Engineering, Pohang University of Science and Technology, Pohang 37673, South Korea

<sup>b</sup> Institute for Convergence Research and Education in Advance Technology, Yonsei University, Seoul, South Korea

<sup>c</sup> College of Engineering and Physical Sciences, University of Guelph, Guelph, ON, Canada



## ARTICLE INFO

This manuscript was handled by Sally Elizabeth Thompson, Editor-in-Chief, with the assistance of Ashok Mishra A, Associate Editor

**Keywords:**

Center-or-volume date  
Pakistan  
Climate change  
Streamflow timing  
CORDEXSouth Asia

## ABSTRACT

Pakistan has experienced seasonal changes of streamflow, causing a lack of available water resources for agriculture. However, understanding of future seasonal changes of streamflow over Pakistan remains limited. This study assessed the past and future changes in streamflow timing along the four major rivers of Pakistan (Upper Indus, Kabul, Jhelum, and Chenab River basins), using observational data and bias-corrected hydrological projections. Firstly, the VIC-river routing model was simulated forced by simulated daily surface and base runoff data from six CORDEX-South Asia regional climate models (1962–2099). Secondly, the minimum and seasonality bias in simulated daily streamflow data were corrected based on observational records. To quantify seasonal changes of the hydrologic regime, half of annual cumulative streamflows (HCSS) and center-of-volume dates (CVDs) were computed from observed and bias-corrected simulated streamflow data. Over 1962–2019, observational records showed a significant decreasing trend in CVD (that is, an earlier onset of the wet season) by a range between  $-4.5$  and  $-12.6$  days across the three river basins, except for Chenab River basin. Bias-corrected hydrologic projections showed decreased CVD across the four study river basins by  $-4.2$  to  $-6.3$  days during the record period (1962–2019). The decreased CVDs ranges from  $-5$  to  $-20$  days in the near future (the 2050–2059 average) and  $-11$  days to  $-37$  days in the far future (the 2090–2099 average). This study reported diverse hydrologic responses to a similar magnitude of near-surface temperature in Pakistan, highlighting a need to develop basin-specific water resources management and policies for climate change adaptation.

## 1. Introduction

The Upper Indus River (UIR) basin provides important water resources for agricultural use, (agricultural, industrial, and domestic) in Pakistan and the northwestern India. The UIR basin includes Chenab, Jhelum, Ravi, Sutlej, and Beas River basins. From the highland areas, the Kabul River is a reach of the UIR at the Tarbela Dam reservoir in Pakistan. Available water resources along these rivers are crucial to support the irrigated agriculture system over the downstream regions that feeds over 200 million people in Pakistan. The agriculture sector in Pakistan contributes to 23 % of the GDP and accounts for 43 percent of the country's labor force (Usman, 2016). Due to strong variability of the regional hydroclimate system in Pakistan, regional communities are vulnerable to hydroclimatic extremes such as drought and flood. In 2010, heavy monsoon rains over Pakistan caused flood inundation over 20 % of the country and inflicted over US\$ 16 billion in economic loss

(Rehman et al., 2016). In 2018, the southern part of Pakistan had persistent precipitation deficits during monsoon season, causing a severe drought (Adnan and Ullah, 2020). Therefore, it is crucial to understand variability and trend of the regional hydroclimate system and the future changes of water availability in Pakistan (Bukhari et al., 2020).

Pakistan is a predominantly agricultural country with the abundant arable land lying within the Indus River basin. There are two agriculture seasons in Pakistan named 'Kharif' and 'Rabi'. The Kharif season refers to summer growing months (May to November), with the major crops cultivated being rice, corn, and cotton. Crop productivity largely depends upon the amount and distribution of rain associated with the monsoon activities during the Kharif season (Ahmed et al., 2019). The Rabi season refers to winter growing months (December through April of the following calendar year), with the major crops being wheat, barley, and millet (Pakistan, 2009). The planting window differs regionally, depending on available water supply, regional climate, and cultivated

\* Corresponding author at: Division of Environmental Science and Engineering, Pohang University of Science and Technology, Pohang 37673, South Korea.  
E-mail address: [jhkam@postech.ac.kr](mailto:jhkam@postech.ac.kr) (J. Kam).

crop type. The major limitation to production is generally the timing and availability of the irrigation water supply, and the efficiency of water on-farm. Due to missing irrigation systems, major crop productivity in the upstream regions of Pakistan is affected by climate variability. Most of this water supply in the UIR basin comes from remote glaciers of the Himalayan and Karakorum mountain ranges while the remainder comes from seasonal rainfall, especially during the monsoon season from July to September. Siddiqui et al. (2012) found that major crops of Pakistan are vulnerable to increased surface temperature, which can cause destructive agricultural losses.

Several studies have reported hydroclimatic changes over South Asia including Pakistan. Shahid and Rahman (2021) found a significant increasing trend of near-surface temperature during springs and summers over the Indus basin and a significant decreasing trend of spring-time precipitation over 1985–2015, raising a concern of a possible change in the drought risk. Mazhar et al. (2016) reported a decline in summertime precipitation in the Himalayas over 1866–2006. Archer (2003) found increased wintertime precipitation over gauge stations of the UIR basin since 1960. Kehrwald et al. (2008) found a rapid retreat of glaciers in the Himalayas, resulting in increased springtime freshwater resources in the downstream regions.

According to climate projections, the Indus and Brahmaputra River basins would experience decreased streamflow in the future (Immerzeel et al., 2010). Khan et al. (2020) found that warmer surface temperature would increase mean annual flow in the future, ranging from 10% to 30% under the future scenarios for the mid-21st century (2041–2070). Spring and winter flows significantly can cause an increased risk of future flood hazards for the UIR basin. Archer et al. (2010) found that there is no evidence of significant reduction in available water resources over the UIR basin due to climate change. However, socio-economic changes would threaten the sustainability of available water resources in the UIR basin. Based on the findings of previous studies, the impact of surface warming-driven changes in streamflow and available water resources on seasonal changes of the hydrologic regime in Pakistan remains uncertain.

Over mountainous regions, the onset of a snow-melting season mainly determines the timing of spring onset and crop planting. Snow and ice-melting processes are sensitive to changes in near-surface temperatures. For example, warmer near-surface temperatures in late winter and early spring accelerates snow and ice-melting processes, causing seasonal changes in soil moistures such as an early onset of spring (Cayan et al., 2001; Kam et al., 2022; Evan and Eisenman, 2021). A wet soil moisture condition in early spring is favorable for floods and a dry soil moisture condition in the following season is favorable for wildfires and heatwaves (Kim et al., 2020). In addition, a previous study (Huss and Hock, 2018) found that streamflow volumes would increase as glaciers melt due to climate change, but that they would reach a “peak water” phase when streamflow volumes would begin to recess as glaciers run out of mass. Qin et al. (2020) found that climate change has altered the regional water balance due to changes in the fraction of precipitation falling as snow and the timing of snowmelt over the Himalayas, Andes, and other mountainous regions. Eventually, these seasonal hydrologic changes can increase the risk of springtime floods and summertime droughts (Kam et al., 2018), causing the crop failure over snow-dominant regions where is more vulnerable to food security.

Seasonal hydrologic changes have been studied mainly over the North American and European regions due to the availability of long-term records of daily streamflow. Over the western U.S. region, observational data showed an earlier spring onset (Schwartz and Reiter, 2000; Menzel and Fabian, 1999; Cayan et al., 2001; Barnett et al., 2005; Dudley et al., 2017; Wasko et al., 2020). A recent study assessed the linkage of wildfire-driven evapotranspiration shift to streamflow timing (Collar et al., 2022). Over the European region, the earlier spring onset caused such seasonal changes, such as leaf unfolding, have advanced by six days whereas autumn events, such as leaf coloring, have been delayed by about five days (Menzel and Fabian 1999) and thus extension

of the growing season (Liu et al., 2018). According to Coupled Model Intercomparison Phase 5 (CMIP5) models, the U.S. region showed geographical variation of trends in winter-spring streamflow timing with a weaker indication of detectable anthropogenic contributions towards the earlier streamflow timing in the western U.S. region. They reported a high sensitivity of WSCT trends over the western part of North America to the record length and climate model bias. In high-mountain Asia, the sensitivity of hydrologic responses (e.g., glacier mass changes) to surface warming are spatially heterogeneous (Kapnick et al., 2014; Sakai and Fujita, 2017). Understanding of hydrologic response, particularly in streamflow timing, to surface warming in high-mountain Asia remain limited (Sharif et al., 2013).

Springtime streamflow of the UIR originates mainly from glacial ice and snowpack in Hindukush, Himalaya, and the Karakorum, one of the largest mountainous regions that contain the world largest hoard of snow and ice masses, except for the Polar Regions (Soncini et al., 2015), while the remainder comes from seasonal rainfall during monsoon season (July to September). Dahri et al. (2021) found that the median annual air temperature for the Indus basin is projected to be increased with a range between 0.8 and 5.7 °C by the end of the 21st century. This near-surface warming trend would result in an increase in the maximum rate of discharge during the wet season in Indus, Kabul, Jhelum, and Chenab Rivers, suggesting a need of critical modification in the strategies to mitigate the adverse effects of future floods and droughts conditions. Archer (2003) found that summertime streamflow volumes are governed by melt of glaciers and permanent snow (thermal control in current summer), melt of seasonal snow (controlled by preceding winter and spring precipitation), and winter and monsoon rainfall. Hasson (2016) found that the median warming of 1 °C or more than 1.5 °C projects the drying of the monsoon (July – September) and the shift of snowpack accumulation/melt season (March – June).

Recent climate change studies over Pakistan have been focused on changes in climatic and hydrologic variables. Yaseen et al. (2020) studied the variability of the hydrometeorological time-series over UIR. They found a warming trend of low altitude stations and an increase in the streamflow was also detected during winter and spring seasons at all hydrological stations, while the annual precipitation showed significant decreasing trend for most of the stations. They also reported annual runoff exhibited significant decreasing trends over Jhelum (five stations) and Indus basin (five stations). Ougahi et al. (2022) found that the increases of the late spring (April through June) water yield were associated with increased annual precipitation and temperature, suggesting a possibility to alter the seasonality of river flows in the Indus River basin. The increasing temperature and precipitation patterns and altering timing of snowfall and glacial melt leads to change in the seasonality of river flows. However, direct studies of seasonal changes in the regional hydrologic response over Pakistan, are limited.

This study aims to investigate past and future changes in streamflow timing in Pakistan from daily streamflow records and simulated daily streamflow data. To achieve it, a river-routing model (Lohmann et al., 1998) is run forced by simulated runoff data from six regional climate models and bias corrections of minimum and seasonality is applied to simulated streamflow data. Our overarching questions are included:

1. Are regional hydroclimate projections reliable to investigate changes in the timing of seasonal streamflow?
2. How much can bias corrections improve simulated daily streamflow?
3. Are the changes in streamflow timing detectable over the past?
4. How are changes in streamflow timing sensitive to future climate scenarios?

The findings of this study will advance the current knowledge of seasonal hydrologic changes in Pakistan and provide a direction for proactive climate change mitigation and preparedness plans for future hydroclimatic extremes such as droughts and floods.

## 2. Data and method

### 2.1. Study region and data

Typically, large river basins are heavily regulated by dams and reservoirs. Pakistan has two major multi-purpose storage reservoirs, Mangla and Tarbela (FAO, 2022). Tarbela and Mangla are located along Upper Indus River and Jhelum River, respectively. Kabul and Chenab Rivers are regulated at Warsak reservoir located in the valley of Peshawar and Marala barrage, respectively. In this study, the four gauge stations along Upper Indus, Kabul, Jhelum, and Chenab River basins are selected as the study basins based on the availability of long-term (greater than 30 years) daily streamflow records, indicating that these stream gages are located upstream of these reservoir control features (Fig. 1). The gaging stations for the four river basins are located at various elevations ranging from 425 to 490 m. The drainage areas of these four basins range between 168,350 (Indus) and 32,282 (Chenab) km<sup>2</sup>. Specific information for the study river basins is provided in Table 1.

This study uses daily streamflow records at the four stations of the study river basins over 1962–2019. Previously, these daily streamflow data have been used by Akhtar et al. (2020) that retrieved the streamflow records through the Global Change Impact Studies Center Pakistan (<http://www.gcisc.org.pk/>). In addition, monthly near surface temperature (NST) and precipitation from the Climate Research Unit (CRU) high-resolution gridded datasets (Harris et al., 2020; <http://crudata.uea.ac.uk/cru/data/hrg/>) were used to compute the regional monthly averages over the corresponding drainage area. These regional monthly averages of NST and precipitation were averaged over January through June to investigate the associations between changes in climatic and hydrologic variables the catchment-scale. The NOAA Climate Data Record of Northern Hemisphere Snow Cover Extent version 1 are used to compute weakly snow cover extent fraction of the Indus river basin (Estilow et al., 2015).

**Table 1**

Geographical information of the gauge stations for the Indus, Kabul, Jhelum, and Chenab River basins.

River	Indus	Kabul	Jhelum	Chenab
Area [km <sup>2</sup> ]	168,350	92,605	33,470	32,282
Elevation [m]	490.20	305.50	341.74	244.70
Longitude [°E]	72.70	71.99	73.63	74.46
Latitude [°N]	34.09	34.01	33.12	32.67

Simulated daily mean surface and base runoff from the Coordinated Regional Climate Downscaling Experiment-South Asia (CORDEX-South Asia) regional climate model simulations are used to estimate the future changes in streamflow timing (Sanjay et al., 2017). Near surface temperature from the CORDEX-South Asia regional climate projections are used to compute changes in near surface temperature in the near and far future (the 2050–2059 and 2090–2099 average, respectively). The CORDEX-South Asia regional climate model projections include the 25-km (0.25-degree) resolution meteorological and land surface data from one ensemble member of historical and future simulations of six models (CanESM2, CNRM-CM5, CSIRO-Mk3-6-0, GFDL-ESM2M, IPSL-CM6A-LR, and MRI-ESM-MR). They provide the Representative Concentration Pathway (RCP) 4.5 and RCP 8.5 future scenario simulations (Giorgi and Gutowski, 2015). The RCP 4.5 and RCP 8.5 scenario runs are stabilized radiative forcing at 4.5 W/m<sup>2</sup> and 8.5 W/m<sup>2</sup> in the year 2100. Previously, the CORDEX-South Asia climate projections have been used to understand the future changes in Hydroclimatology over the Himalayan region, particularly Indian monsoon system (Choudhary and Dimri, 2018; Raju et al., 2015), hydroclimatic extremes (Suman and Maity, 2020; Rai et al., 2019), and water security (Dubey et al., 2020).

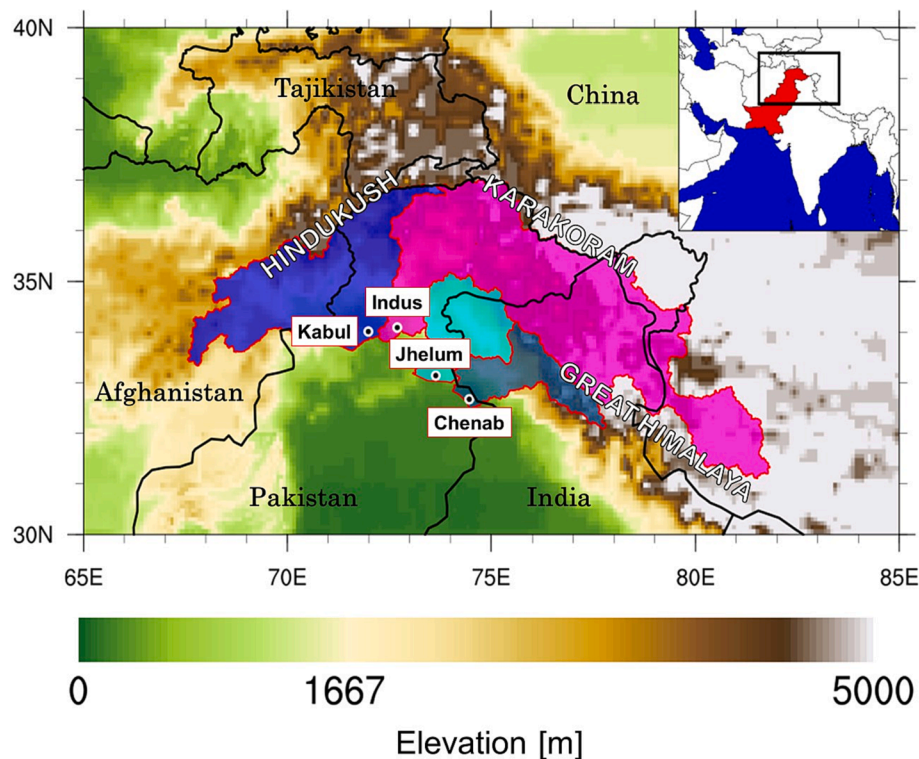


**Fig. 1.** Study River basins of Chenab (dark green), Indus (pink), Jhelum (sky blue), and Kabul (blue) river. Black dots depict the geographical locations of the corresponding gage stations. Background colors and a color bar depict elevations above sea level. (For interpretation of the references to color in this figure legend, the reader is referred to the web version of this article.)

## 2.2. Methods

### 2.2.1. Simulated streamflow using a river routing model

To simulate daily streamflow at four river basins in Pakistan, the Variable Infiltration Capacity-River Routing Model (VIC-RRM; Lohmann et al., 1998) was run forced by simulated daily total surface and base runoff data from six CORDEX-South Asia regional climate projections. The VIC-RRM has been developed to resolve a linearized version of the Saint-Venant equations (Lohmann et al., 1996). The original (gauge-based) and modified (grid-based) versions of this model has been used and validated in many previous studies at various spatial scales (Nijssen et al., 1997; Sheffield et al., 2013; Yuan et al., 2015).

In this study, the grid-based streamflow routing model was used since it can be simulated at the large spatial scale that is consistent to the scale of the CORDEX regional climate projections. The source code for the gridded version of VIC-RRM is available upon request to the corresponding author. The VIC-RRM simulates daily streamflow via a simple linear transfer function, assuming that total runoff (surface + base runoff) at each grid cell (herein, 25-km by 25-km grid cells) is transferred into at least one of the eight adjacent grid cells (Lohmann et al., 1996). In addition, the runoff transport process is assumed to be linear and time-invariant (Lohmann et al., 1998) and the causality and the impulse response functions between grid cells are nonnegative (Duband et al., 1993; Littlewood and Jakeman 1994). Based on the 25-km digital elevation model (DEM) data, first topography information including the slope, stream order, and flow direction were calculated and then water transport velocity, the drainage area of this grid cell and the distance to next grid cell. Then, daily streamflow at each grid cell was calculated using simulated daily runoff data from historical (1962–2005) and future (2006–2099) projections of the CORDEX-South Asia regional climate models.

### 2.2.2. Bias correction of minimum and seasonality

Bias correction methodologies are necessarily applied to simulated daily streamflow data due to the well-known climate model bias for hydrologic studies (Kam et al., 2018; Bennett et al., 2022; Meresa et al., 2022). In this study, minimum bias correction is applied to simulated streamflow data, instead of mean bias correction, to minimize negative values during the low flow season. Simulated daily streamflow were subtracted by the minimum of simulated streamflow over 1962–2005, and then were multiplied by the ratios of the standard deviations of observed to simulated daily streamflow for the corresponding calendar year. Then, they were added by the observed minimum streamflow value over 1962–2005 (Eq. (1)). It is worth noting that daily streamflow on the last day of February of lunar years was added to daily streamflow on the previous day to have the constant time step of each year ( $t = 1, \dots, 365$ ).

$$Q_{corr\_minj}(t) = Q_{obs\_min} + \frac{Std(Q_{obsj})}{Std(Q_{simj})} \times (Q_{simj}(t) - Q_{sim\_min}(t)) \quad (1)$$

where  $Q_{corr\_minj}(t)$  is minimum bias-corrected simulated daily streamflow for a day,  $t$  ( $t = 1, \dots, 365$ ), of the calendar year,  $j$  ( $j = 1962, \dots, 2005$ ),  $Q_{obs\_min}$  and  $Q_{sim\_min}$  are the minimum values from observed and simulated streamflow, respectively, over 1962–2005, and  $Std(Q_{obsj})$  and  $Std(Q_{simj})$  are the standard deviations of observed and simulated streamflow, respectively, for a calendar year,  $j$ .

In this study, a simple weighting bias correction by a ratio of observed to simulated standard deviations was used to resolve non-stationarity of the hydrologic system, particularly in the future (Kam et al., 2018), instead of the quantile machanig bias correction that is based on the stationarity of the hydrologic system and is appropriate for reconstruction of streamflow data over the past. After the minimum bias correction, the annual total streamflow is computed by summing daily streamflow during a calendar year,  $j$  (Eq. (2)).

$$Q_{corr\_minj} = \sum_{t=1}^{365} Q_{corr\_minj}(t) \quad (2)$$

Next, the cumulative percentages of minimum bias-corrected daily streamflow for each calendar year were computed (Eq. (3)).

$$\Delta_j(t) = 100 \times \frac{\sum_{t=1}^t Q_{corr\_minj}(t)}{Q_{corr\_minj}} \quad (3)$$

where  $\Delta_j(t)$  is the cumulative percentage of daily streamflow on a day,  $t$ , of the calendar year,  $j$ .

In this study, daily seasonality bias,  $\delta(t)$ , was defined as the long-term (1962–2005) averages of the difference between daily cumulative percentages of observed and simulated daily streamflow (Eq. (4); (c) in Fig. 2).

$$\delta(t) = \sum_{j=1962}^{2005} \left( \frac{P_{obsj}(t) - P_{simj}(t)}{44} \right) \quad (4)$$

where the  $P_{simj}(t)$  and  $P_{obsj}(t)$  are the cumulative percentiles of raw simulated and observed daily streamflow on the  $t^{\text{th}}$  day of the  $j^{\text{th}}$  calendar year, respectively.

We assumed that the model discrepancies (herein, seasonality bias) with observational records are constant over time (Ho et al., 2012). For example, the errors in the relationship between the distribution of observed and simulated daily streamflow are the same in the past and future. This assumption allows correction of future simulated streamflow to be obtained by adding the seasonality bias to the cumulative daily streamflow percentage. After computing the seasonality bias, the cumulative daily streamflow ( $Q_{corr\_sea_j}(t)$ ) is disaggregated at the daily scale through Eqns. (5)&(6).

$$Q_{corr\_sea_j}(t) = \frac{\Delta_j(t) + \delta(t)}{100} \times Q_{corr\_minj} \quad (5)$$

$$Q_{corrj}(t) = \begin{cases} Q_{corr\_sea_j}(t), & \text{if } t = 1 \\ Q_{corr\_sea_j}(t) - Q_{corr\_sea_j}(t-1), & \text{if } t > 1 \end{cases} \quad (6)$$

After the minimum and seasonality bias correction, few negative values are found from the corrected simulated streamflow data. These negative values are around 0.5–2 % for all the basins during the overlapping period (1962–2005) and less than 1 % for all the basins in the near and far future. To compute the CVD values, negative streamflow data are replaced with the seven-day average values centering on the dates with a negative value (−3 and +3 days).

### 2.2.3. Calculation of streamflow timing

Streamflow timing have been often measured by half-flow dates as the dates on which half of the annual/seasonal total streamflow has passed (Court, 1962); (Hodgkins et al., 2003). In this study, half of cumulative daily streamflow ( $HCS_j$ ) and the center-of-volume dates (CVD<sub>*j*</sub>) for a calendar year,  $j$ , were computed using Eqns. (7) and (8), respectively (Fig. 3).

$$HCS_j = \frac{\sum_{t=k}^{365} q_j(t)}{2} \quad (7)$$

$$CVD_j = \min[m] \sum_{i=k}^m q_j(t) \geq HCS_j/2 \quad (8)$$

where  $m$  is the  $m^{\text{th}}$  days of the calendar year  $j$ , when the cumulative daily streamflow from the first day to the  $m^{\text{th}}$  day exceeds  $HCS_j$  first time within the calendar year,  $j$ .

To evaluate the impact of bias correction on the performance, two common goodness-of-fit metrics (Nash-Sutcliffe Efficiency (NSE) and Kling-Gupta Efficiency (KGE) of bias-corrected streamflow data were

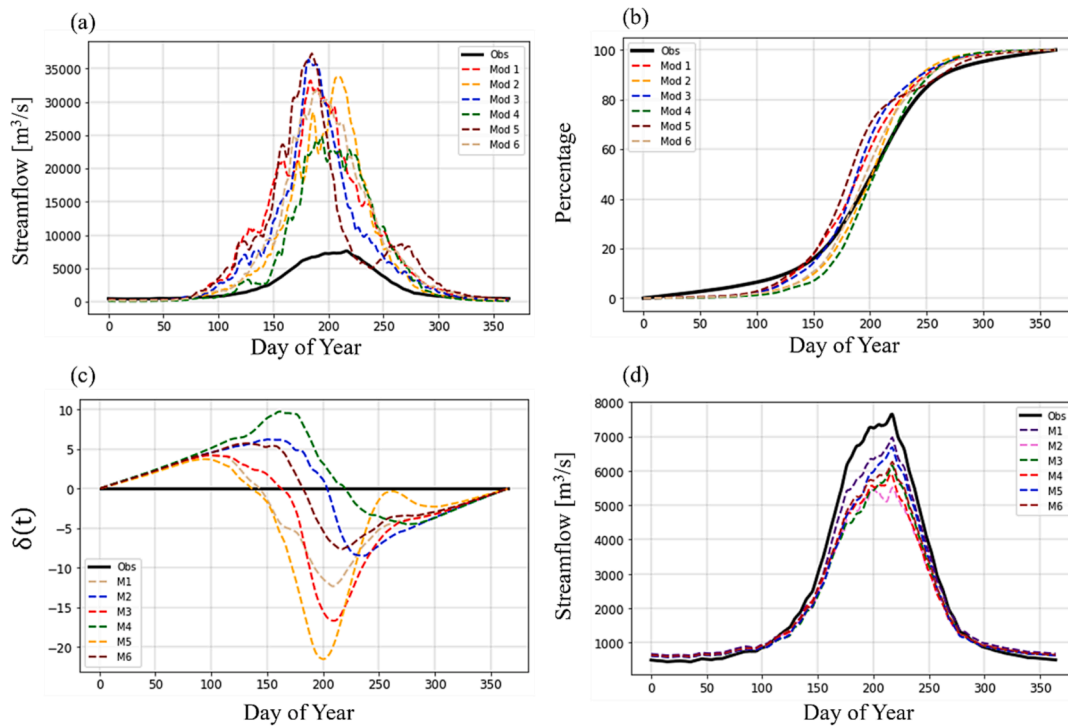


**Fig. 2.** Seasonality bias correction for Indus basin. Black solid and colored (red, yellow, blue, green, purple, and brown) dash lines depict seasonality (the 1962–2005 averages) (a), cumulative percentages (b), and the difference between the cumulative daily percentages (c) of observed and raw simulated streamflow of observed and raw simulated daily streamflow from six CORDEX-South Asia regional climate models. In (d), black solid and colored (red, yellow, blue, green, purple, and brown) dash lines depict cumulative percentages of observed and bias-corrected daily streamflow from the six climate models. (For interpretation of the references to color in this figure legend, the reader is referred to the web version of this article.)

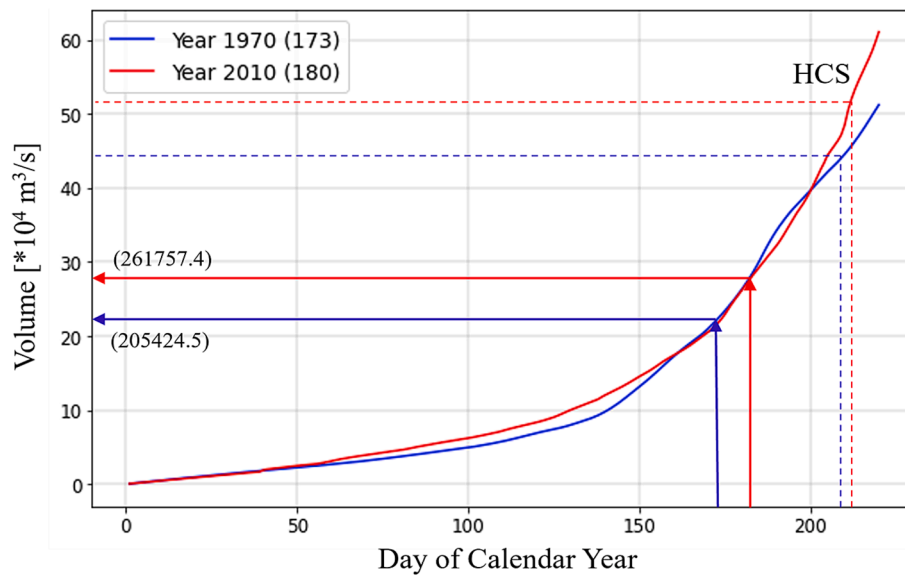


**Fig. 3.** Cumulative daily streamflow of Indus River from January to June in 1970 (blue line) and 2010 (red line). Blue and red arrows depict the half of HCSs (y-axis) and CVDs (x-axis) in 1970 and 2010, respectively. (For interpretation of the references to color in this figure legend, the reader is referred to the web version of this article.)

reported in Section 3.1. NSE is calculated as one minus the ratio of the error variance of the modelled time series to the variance of the observed time-series (Eq. (9)). While a perfect model has one of NSE, a model that has the same prediction skills than the average of the mean observed values has zero of NSE.

$$NSE = 1 - \frac{\sum_{j=1962}^{2005} \sum_{t=1}^{365} Q_{obsj}(t) - Q_{corrj}(t)}{\sum_{j=1962}^{2005} \sum_{t=1}^{365} Q_{obsj}(t) - \bar{Q}_{obsj}} \quad (9)$$

KGE has been increasingly used for model calibration and evaluation (Eq. (10)) since it combines the three components of NSE (correlation, variability bias and mean bias) in a balanced way (Eq. (10); Knoben

et al., 2019). While a perfect model has one of KGE, a model that has the same prediction skills than the average of the mean observed values has  $-0.41$  of KGE.

$$KGE = 1 - \sqrt{(r - 1)^2 + (\beta - 1)^2 + (\gamma - 1)^2} \tag{10}$$

where  $r$  is the Pearson correlation coefficient between observed and bias-corrected streamflow,  $\beta$  is the ratio of the long-term averages of bias-corrected streamflow to observed streamflow (bias ratio), and  $\gamma$  is the ratio of coefficients of variation of bias-corrected streamflow to observed streamflow (variability ratio).

2.2.4. Mann-Kendall test

In this study, the non-parametric Mann-Kendall (MK) test (Mann, 1945; Kendall, 1975; Lettenmaier et al., 1994) was conducted to check the significance of the past trend of hydroclimate variables over the four study river basins. In this study, the trends were evaluated at the significant level ( $\alpha$ ), 0.05 and 0.1 for two-tail test. The MK test determines whether a time series of streamflow has a statistically significant (monotonic) trend of streamflow. In this study, the Python module 'pyMannkandal' is used to compute MK statistics (Hussain and Mahmud, 2019). This package reports the sign of the trend (increase/decrease)

and statistical significance (True/False) based on multiple statistics, including p-value, z (normalized test statistics), Tau (Kendall tau), s (Mann-Kendall score) and its variance, slope (Sen estimator/slope), and an intercept of Kendall robust line. A more detailed description of the MK test is found in (Kumar et al 2009).

The original MK test does not account for autocorrelation in the data when the significance of a monotonic trend is evaluated. Different versions of the MK test have been previously proposed to account for short- and long-term consistency. These versions were applied to remove the autocorrelation structure (Kam and Sheffield, 2016) and long-term persistency (Kumar et al., 2009) in observed streamflow data. In this study, the results from the classical MK test are reported because we found that time series of CVDs are serially independent (not shown).

3. Results

3.1. Evaluation of bias-corrected streamflow

Fig. 4 shows Nash-Sutcliffe Efficiency (NSE) and Kling-Gupta Efficiency (KGE) metrics of simulated and bias-corrected streamflow data against observed streamflow data. Raw simulated streamflow data over all the four basins show negative NSE values with different magnitudes

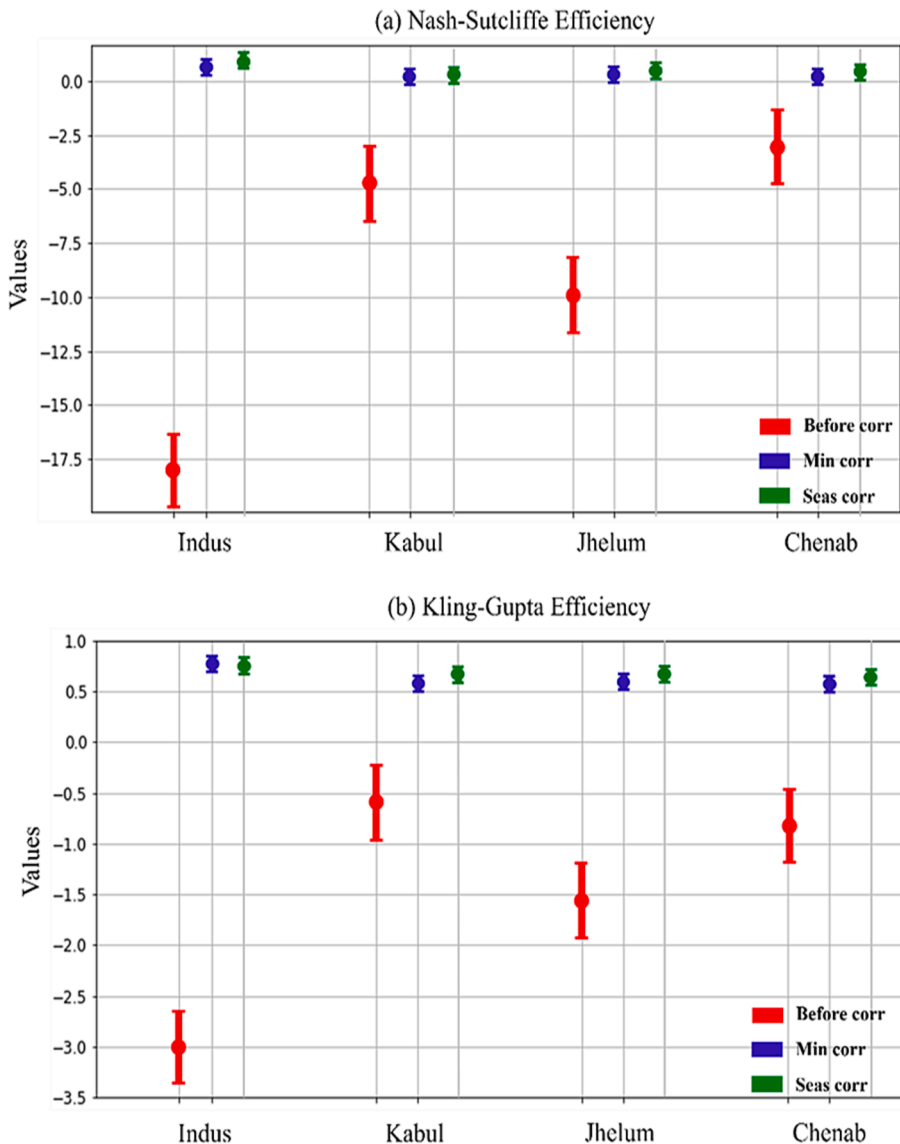


Fig. 4. Goodness-to-fit performance of simulated streamflow: Nash-Sutcliffe Efficiency (NSE) (a) and Kling-Gupta Efficiency (KGE) (b) for the four river basins. Red, blue, and green colored lines depict NSE and KGE values of raw simulated, minimum bias-only corrected, and minimum and seasonality bias corrected streamflow and the circle on center shows the mean value for each, respectively. (For interpretation of the references to color in this figure legend, the reader is referred to the web version of this article.)

(Indus (1st largest negative NSE value), Jhelum (2nd), Kabul (3rd) and Chenab River basins (4th)). Generally, the goodness-to-fit metrics are significantly higher over all the four river basins after the minimum bias correction. The impacts of seasonality bias correction after minimum bias correction are various across the metrics and study basins. The NSE shows significant improvement of the performance after seasonality bias corrections across the study basins. The KGE shows no significant improvement over Indus and Kabul River basins while Jhelum River basin still show a significantly higher KGE value after seasonality correction. The results are consistent with those from the minimum bias correction after the seasonality bias correction, implying that the order of the bias corrections has no impact on uncertainty reduction. Therefore, the minimum bias correction is a key contribution of uncertainties reduction in simulated streamflow with a minor impact of the seasonality bias correction across the basins. It also implies that a calibration strategy design is carefully designed when simulated streamflow data from climate models are used for regional hydrologic studies and a robust goodness-to-fit assessment is required through multiple verification metrics.

### 3.2. Seasonality and past changes in hydroclimatology over Pakistan

Fig. 5 shows the seasonality of the regional averages of NST and precipitation over the drainage areas of the study river basins. Overall, the NST shows a boreal seasonal cycle with a peak month in July. The

Indus River basin has only four (June through September) months when the NST is above the freezing temperature of water ( $0^{\circ}\text{C}$ ). Other three river basins have seven (Kabul) to nine months above  $0^{\circ}\text{C}$ . This is because the corresponding drainage area to the Indus River basin covers high-elevation regions covering the Hindukush, Karakorum, and Himalaya ranges (Fig. 1). The seasonality of precipitation shows two peak wet seasons within the calendar year in early spring (March) and summer (July and August). These two peaks shows maximum value of precipitation during the two crop growing seasons of Pakistan, the Rabi (December–April) and Kharif (May–November) seasons. The Indus River basin has the lowest precipitation among the study river basins and shows a slightly higher peak of summertime (July–August) precipitation than that of springtime (February–April) precipitation.

The Kabul River basin has the 2nd lowest precipitation with low summer precipitation, indicating a weak impact of Indian monsoon due to the tropospheric anomalous high over the western central Asia (Saeed et al., 2011). Jhelum and Chenab River basins have a common seasonality of precipitation with a much higher peak in July and August when Indian monsoon is active.

The sign of observed trends in HCSs were negative, but insignificant, for all four river basins (Table 2). Bias-corrected streamflow data show consistency with half volumes from observational records for the four river basins, that is, the observed half volumes are placed between the minimum and maximum of half volumes from six CORDEX models over most of 1962–2005 (Fig. 6). Over the Indus River basin, observed half

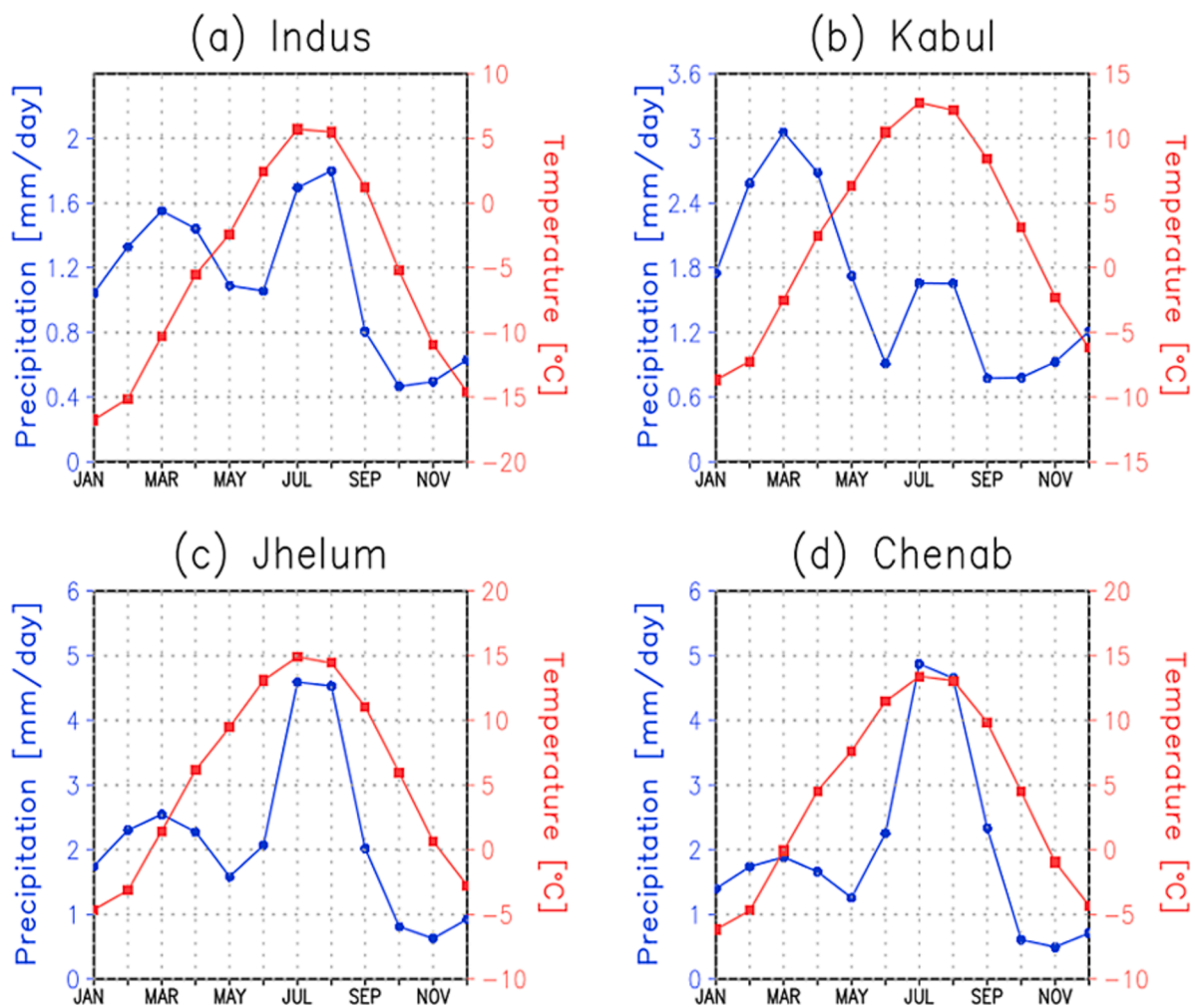


Fig. 5. Seasonality of precipitation (blue line with circle markers, mm/day) and near surface temperature (red line with square markers,  $^{\circ}\text{C}$ ) over Indus (a), Kabul (b), Jhelum (c), and Chenab (d) River basins. Seasonality is computed from the averages of precipitation and near-surface temperature over 1962–2019. (For interpretation of the references to color in this figure legend, the reader is referred to the web version of this article.)

**Table 2**

Sen slopes of observed near-surface temperature, precipitation, CVD, and first half volume for the four river basins. Near-surface temperature and precipitation are the corresponding drainage area averages of the mean temperature between January through June. Numbers in **bold** and *italic* depict a statistically significant trends from a non-parametric Mann-Kendall' test at the significant level, 0.05 and 0.1, respectively, for two-tail test.

		Indus	Kabul	Jhelum	Chenab
NST	Slope [°C/year]	<b>+0.030</b>	<b>+0.023</b>	<b>+0.021</b>	<b>+0.024</b>
	p-value	4.55e-09	8.00e-05	9.45e-05	5.61e-07
Precipitation	Slope [mm/day/year]	+0.003	<i>+0.013</i>	+0.003	+0.004
	p-value	0.018	0.033	0.447	0.545
CVD	Slope [day/year]	<b>-0.107</b>	<b>-0.166</b>	<b>-0.222</b>	<b>-0.208</b>
	p-value	0.035	0.005	0.002	0.056
HCS	Slope [m <sup>3</sup> /year]	-0.015	-0.018	-0.009	-0.013
	p-value	0.375	0.307	0.502	0.354

volumes are near or at the maximum of simulated half volumes and show higher half volumes in 1960s than the maximum of simulated half volumes, that is, simulated half volumes are inconsistent with observed half volumes. Over the Kabul and Chenab River basins, observed half volumes are near or at the minimum of simulated half volumes and higher half volumes.

For the four study river basins, observed CVDs are generally between late April through early June (100th through 180th day of the calendar year) and show a decreasing trend over 1962–2019 (Fig. 7). Bias-corrected streamflow data show consistency with observed CVDs for the four river basins over 1962–2005. Observed CVDs are close to the minimum of bias-corrected CVDs from the six CORDEX models for Jhelum River basin while observed CVDs are close to the average of the six CORDEX models for the rest of the three study river basins. Over

1962–2019 observed CVD values have become earlier by about 5, 9.1, 12.6, and 12.5 days for Indus, Kabul, Jhelum, and Chenab River basins, respectively, indicating an earlier onset of the spring season in the recent decades.

The relationship of observed CVDs with the monthly minimum near surface temperature in March (May) are examined over Indus, Chenab, and Jhelum River basins (Kabul River basin) when their negative correlation is strongest (not shown). The results show that the NST has increased over 1962–2019 by about 2.0 °C across the study basins, implying that the decreasing trend of CVD can be related to early melting of snow cover and glaciers over land due to the increased minimum NST. However, it requires further studies about precipitation-snow cover-NST interactions.

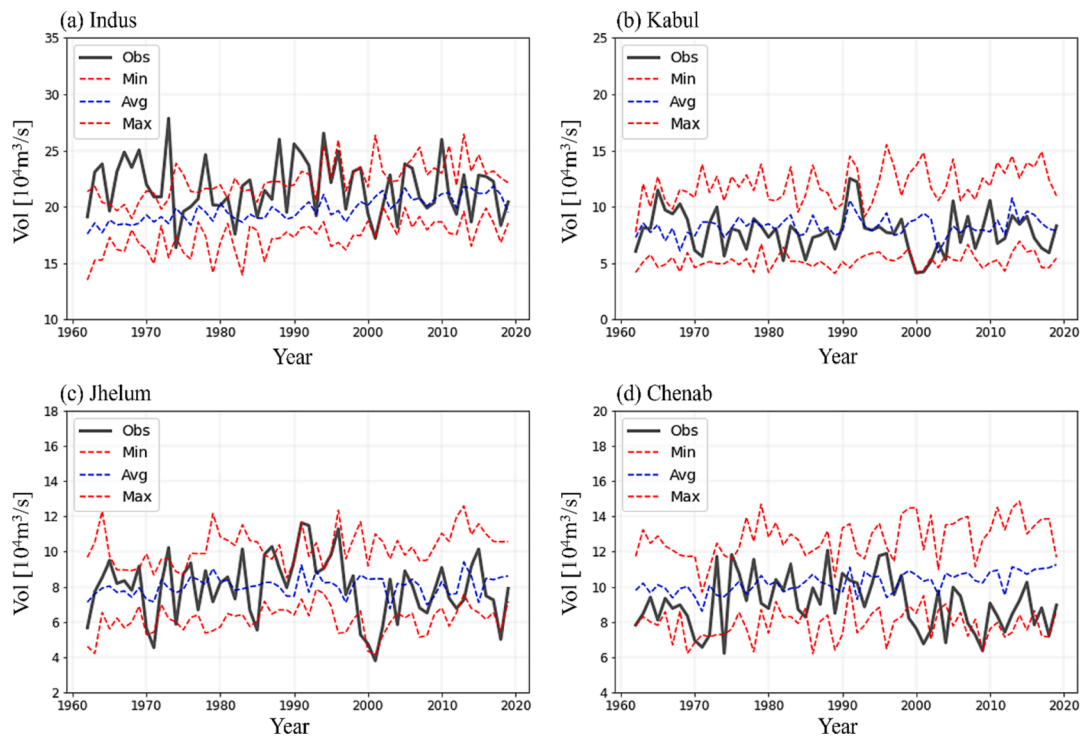


**Fig. 6.** Annual time series of half of observed (black solid lines) and simulated HCSs (dashed lines) for Indus (a), Kabul (b), Jhelum (c), and Chenab (d) River basins. Blue and red dashed lines depict of the average and minimum/maximum of half of simulated HCSs of the six CORDEX-South Asia regional climate models. (For interpretation of the references to color in this figure legend, the reader is referred to the web version of this article.)

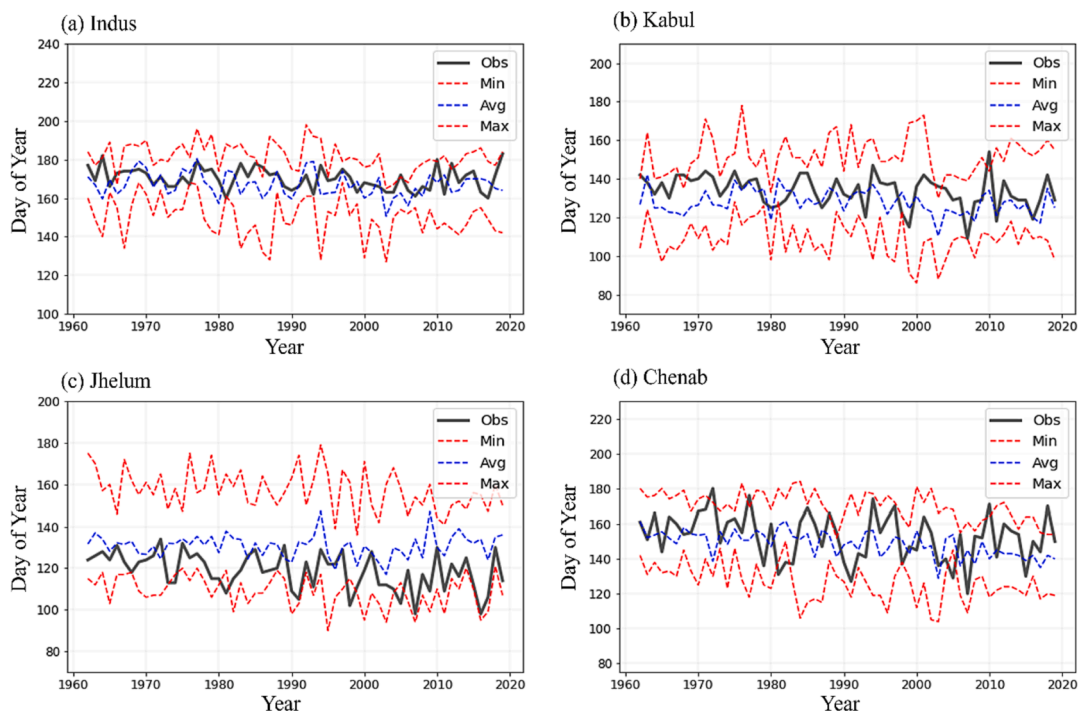


Fig. 7. Same as Fig. 6, except for center-of-volume dates (CVDs).

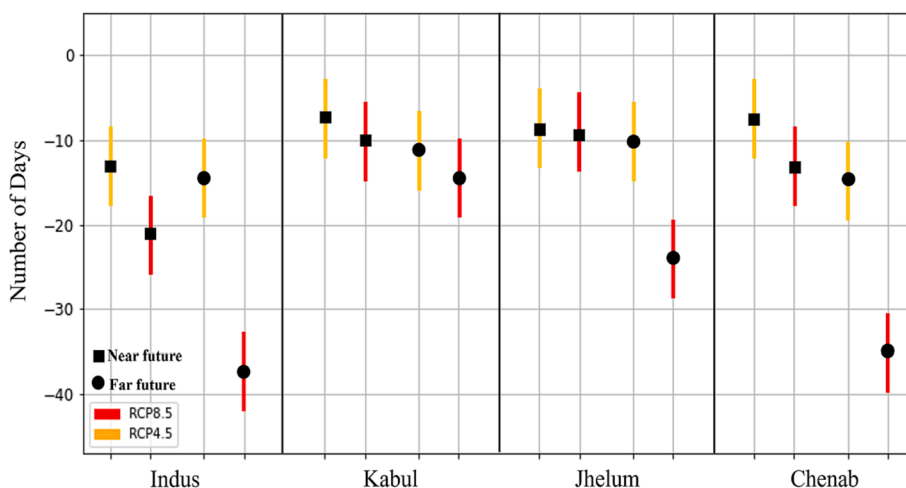


Fig. 8. Future changes in CVDs from bias-corrected daily streamflow relative to the 1962–2019 climatology. Square and circle markers depict changes of CVDs in the near (2050–2059) and far (2090–2099) future, respectively. Red and orange box plots depict future changes in CVDs from the RCP8.5 and RCP4.5 future scenarios, respectively. (For interpretation of the references to color in this figure legend, the reader is referred to the web version of this article.)

### 3.3. Outlook of changes in CVD

Fig. 8 shows the future changes in CVDs for near and far future (the averages over 2050–2059 and 2090–2099, respectively). The CVDs from corrected streamflow data shows that CVDs become earlier over all the four study basins in the future with spatial differences in the magnitude of the CVD changes. Overall, the four study river basins show earlier CVDs ranging from 8 to 13 days and 11 to 15 days in 2050s and 2090s, respectively, under the RCP4.5 scenario. The Indus and Chenab River basins show earlier CVDs by 22 and 16 days, respectively, in 2050s of the RCP8.5 scenario while the Kabul and Jhelum River basins show earlier CVDs by 10 days. In 2090s of the RCP8.5 scenario, the Indus and Chenab River basins show earlier CVDs by 37 and 32 days, respectively, and the Kabul and Jhelum River basins show earlier CVDs by 15 and 24 days, respectively.

From the future CORDEX-South Asia climate projections, the future changes in near surface temperatures (NST) are further examined as a potential cause of the future CVD changes for the study river basins (Fig. 9). There is a general tendency of NST that near surface is warmer by above 2 °C and 5 °C in the near and far future, respectively, across the study river basins. The results indicate that the hydrologic response to a similar magnitude of near-surface warming varies, depending on regional climate and the geographical characteristics of the catchment on interest.

### 4. Discussion

According to the bias-corrected CORDEX climate projections, observed decreasing trends of the CVD will likely continue. This study found spatial variations of the magnitude of CVD changes across the

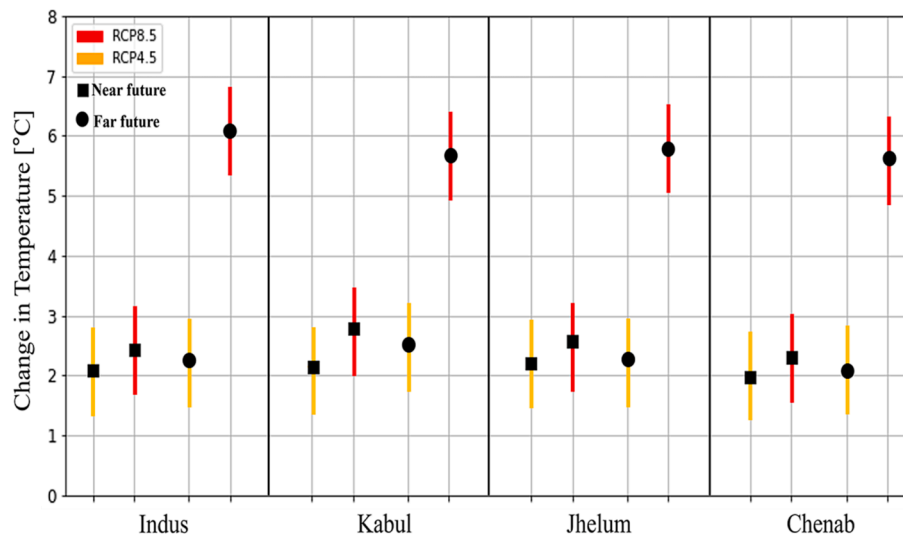


Fig. 9. Same as Fig. 8, except for changes in near-surface temperature anomalies relative to the 1962–2019 climatology.

study river basins given a similar magnitude of near surface warming in the future. Different hydrologic responses can be related to regional precipitation seasonality and geographical characteristics, including location, elevation, land cover, and slope. For example, mountainous regions have snowfall, which are stored in a form of snowpack during the winter months. In the early spring months, snowpacks are melted during the spring months when the surface temperature is above the freezing temperature. The geographical characteristics (e.g., slope aspect) will strengthen or weaken the change of surface warming on the rate of snow-melting processes, which can lead to diversity in the seasonal changes in streamflow timing over mountainous areas like our study basins (Kapnick et al., 2014; Kang et al., 2016; Kam et al., 2018; Gordon et al., 2022), except for Kabul River basin (an arid/semi-arid region).

If precipitation shows no significant trend, changes in the seasonality of streamflow is strongly correlated with changes in the speed of snow melting over snow-dominant regions like the Upper Indus River (e.g., change in the fraction of snow cover areas; Fig. 10). However, current regional and global climate models have a poor representation of snow melting processes due to the coarse resolution of the models and missing the detailed physics for snow-melting processes in the coarse resolution models. Therefore, higher resolution models that include detailed snow-melting processes is required for reliable regional hydrologic projections

(Du et al., 2022; Meresa et al., 2022).

Similar results were also found by Ougahi et al. (2022), using a semi-distributed hydrologic model, Soil and Water Assessment Tool. They found that the climate change has implications for the water resources by a combination of changes in temperature and precipitation patterns, resulting in seasonal changes of river flows. These changes will affect the crop productivity over Pakistan. A recent study (Dahri et al., 2021) on climate and hydrologic regimes of high-altitude Indus basin found that the mean air temperature is projected to increase further between 0.8 and 5.7 °C by the end of 21st century. The inflow of Indus-Tarbela is likely to increase compared to Kabul, Jhelum and Chenab River inflows. Furthermore, a substantial increase in the magnitude of peak flows and one-month earlier attainment is also projected for all river gauges. However, this study found a non-significant trend of the mean precipitation for January through June and the 1st half volume since 1962, which need a further investigation for an emergence time of the trends in hydroclimatic variables during winters and springs over the study regions.

Global climate change affects the regional climate and hydrologic systems differently. This study was focused on past and future seasonal changes over Pakistan as a regional hydrologic response of the high mountainous region to global climate change. This study found a significant change of streamflow timing over Pakistan during the late

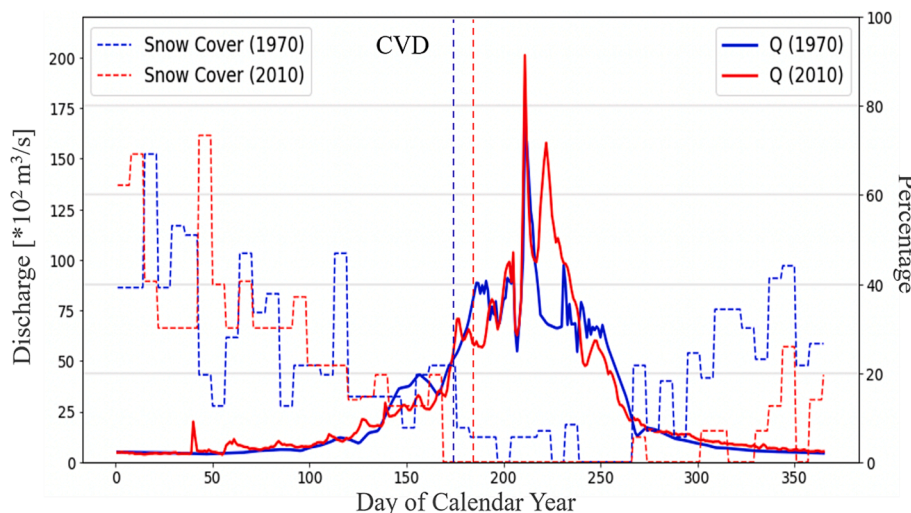


Fig. 10. Daily discharges of the Indus River basin in 1970 (blue solid line) and 2010 (red solid line). Blue and red dash lines depict weekly percentages of snow cover area from NOAA Climate Data Record (CDR) of Northern Hemisphere (NH) Snow Cover Extent (SCE) version 1 in 1970 and 2010, respectively. Percentages of the snow cover area are shown in the secondary y-axis (right). (For interpretation of the references to color in this figure legend, the reader is referred to the web version of this article.)

winter and early spring, which can affect crop yield with the current planting and cultivating schedules. The proposed methods are applicable to other high mountainous Asian countries where the long-term daily streamflow data is available. Recently, the reanalysis products, such as ECMWF Reanalysis version 5 (ERA5; Hersbach et al., 2020), provide global long-term hydrologic variables, leading to research opportunities to explore the past seasonal change of hydrologic systems around the world (Bain et al., 2022). New global datasets are available to extend the proposed bias-correction methods to evaluate changes in streamflow timing in mountainous regions including the Himalayas, Andes and other mountainous regions where are susceptible to climate change (Mishra, 2015; Immerzeel et al., 2020). In addition, a new phase of the CORDEX project (Gutowski Jr. et al., 2016) provides the relatively high resolution hydroclimatic projection, which also enable us to explore the climate change impact on regional hydrologic response via the proposed methods in this study.

The findings of this study were based on the upstream gauge stations to avoid human disturbance. The current water engineered systems in the downstream regions can mitigate the impact of climate change, but understanding of to what extent they can mitigate remain unknown. This study suggests the need to further investigate the capacity of the current water engineered systems in the downstream regions for climate change adaptation and mitigation. This study also alerts other high mountain Asian countries of the need to investigate the need to upgrade water engineer systems and water resources management planning.

## 5. Conclusions

This study highlights the diverse hydrologic responses in Pakistan to +2/+6 °C near surface warming, which can cause changes in the risk of climatic extremes, such as droughts and floods. This study informs a need for proactive climate adaptation planning to meet the regional and national forthcoming needs and basin-based strategies for sustainability of water resources systems in Pakistan. To mitigate efficiently the impact of climate change in Pakistan, further studies for actual causes of the decrease in the CVDs and their impacts on the risk of climatic extremes in the following summer months are warranted.

Furthermore, the two crop growing seasons of Pakistan, Rabi (agriculture crops sown in winter and harvested in the spring) and Kharif (domesticated plants cultivated and harvested during the rainy season) will be altered due to this change in the CVD and half volume values in future. During the Kharif season, streamflow is dominated by snowmelt-based flows in early spring and monsoon rainfall in summer while precipitation is mostly in the form of snowfall and the baseflow is from groundwater during the Rabi season. As the streamflow cresting is shifting earlier, the definitions of these seasons will likely change. This study suggests the need to update of the current crop planning schedule for climate change adaptation.

## CRedit authorship contribution statement

**Shahid Ali:** Methodology, Data curation, Formal analysis, Investigation, Validation, Visualization, Writing – original draft, Writing – review & editing. **Byeong-Hee Kim:** Visualization, Writing – review & editing. **Taimoor Akhtar:** Data curation, Writing – review & editing. **Jonghun Kam:** Conceptualization, Funding acquisition, Methodology, Supervision, Writing – review & editing.

## Declaration of Competing Interest

The authors declare the following financial interests/personal relationships which may be considered as potential competing interests: Kam, Jonghun reports financial support was provided by National Research Foundation of Korea. Ali, Shahid reports financial support was provided by National Research Foundation of Korea.

## Data availability

The data used in this study are available at the following public websites: CORDEX data at <https://esg-dn1.nsc.liu.se/search/cordex/>. Daily streamflow data of four rivers in Pakistan was obtained upon request to the corresponding author or the Pakistan Water and Power Development Authority (<https://www.wapda.gov.pk>). Daily raw and bias-corrected observed and simulated streamflow data of four rivers in Pakistan are available at <https://doi.org/10.7910/DVN/J3CXG1>. NST and Precipitation data at <https://esg-dnl.nsc.liu.se/search/cordex/>.

## Acknowledgements

We acknowledge the agencies that support the CORDEX South Asia system, and we thank the CORDEX South Asia-participant climate modeling groups for producing and making available their model output. This study was supported by the National Research Foundation of Korea (NRF-2021R1A2C1093866). Shahid Ali was supported by the Globla Korea Scholarship (GKS) Program of the National Institute for International Education (NIIED), a branch of the Ministry of Education in the Republic of Korea.

## References

- Adnan, S., Ullah, K., 2020. Development of drought hazard index for vulnerability assessment in Pakistan. *Nat. Hazards* 103, 2989–3010. <https://doi.org/10.1007/s11069-020-04116-3>.
- Ahmed, K., Shahid, S., Wang, X., Nawaz, N., Khan, N., 2019. Spatiotemporal changes in aridity of Pakistan during 1901–2016. *Hydrol. Earth Syst. Sci.* 23 (7), 3081–3096. <https://doi.org/10.5194/hess-23-3081-2019>.
- Akhtar, T., Mushtaq, H., Hashmi, M.-Z.-R., 2020. Drought monitoring and prediction in climate vulnerable Pakistan: Integrating hydrologic and meteorologic perspectives. *Hydrol. Earth Syst. Sci. Discuss.* 1–29.
- Archer, D., 2003. Contrasting hydrological regimes in the upper Indus Basin. *J. Hydrol.* 274, 198–210.
- Archer, D.R., Forsythe, N., Fowler, H.J., Shah, S.M., 2010. Sustainability of water resources management in the Indus Basin under changing climatic and socio-economic conditions. *Hydrol. Earth Syst. Sci.* 14, 1669–1680.
- Bain, R.L., Shaw, M.J., Geheran, M.P., Tavakoly, A.A., Wahl, M.D., Zsoter, E., 2022. Intercomparison of global ERA reanalysis products for streamflow simulations at the high-resolution continental scale. *J. Hydrol.* 128624.
- Barnett, T.P., Adam, J.C., Lettenmaier, D.P., 2005. Potential impacts of a warming climate on water availability in snow-dominated regions. *Nature* 438, 303–309.
- Bennett, A., Stein, A., Cheng, Y., Nijssen, B., McGuire, M., 2022. A process-conditioned and spatially consistent method for reducing systematic biases in modeled streamflow. *J. Hydrometeorol.*
- Bukhari, S.A.A., Ahmad, B., Tahir, A.A., 2020. Exploring climate change impacts during the first half of the 21st century on flow regime of the transboundary Kabul River in the Hindukush region. *J. Water Clim. Change* 1521–1538.
- Cayan, D.R., Kammerdiener, S.A., Dettinger, M.D., Caprio, J.M., Peterson, D.H., 2001. Changes in the onset of spring in the western United States. *Bull. Am. Meteorol. Soc.* 82, 399–416.
- Choudhary, A., Dimri, A.P., 2018. Assessment of CORDEX-South Asia experiments for monsoonal precipitation over Himalayan region for future climate. 50, 3009–3030. <https://doi.org/10.1007/s00382-017-3789-4>.
- Collar, N.M., Saxe, S., Ebel, B.A., Boden, K.S., Rust, A.J., Hogue, T.S., 2022. Linking fire-induced evapotranspiration shifts to streamflow magnitude and timing in the western United States. *J. Hydrol.* 612, 128242.
- Court, A., 1962. Measures of streamflow timing. *J. Geophys. Res.* 1896–1977 (67), 4335–4339. <https://doi.org/10.1029/JZ067i011p04335>.
- Dahri, Z.H., Ludwig, F., Moors, E., Ahmad, S., Ahmad, B., Ahmad, S., Riaz, M., Kabat, P., 2021. Climate change and hydrological regime of the high-altitude Indus basin under extreme climate scenarios. *Sci. Total Environ.* 768, 144467.
- Du, X., Silwal, G., Faramarzi, M., 2022. Investigating the impacts of glacier melt on stream temperature in a cold-region watershed: coupling a glacier melt model with a hydrological model. *J. Hydrol.* 605, 127303.
- Duband, D., Oblad, C.h., Rodriguez, J.Y., 1993. Unit hydrograph revisited: an alternate iterative approach to UH and effective precipitation identification. *J. Hydrol.* 150, 115–149. [https://doi.org/10.1016/0022-1694\(93\)90158-6](https://doi.org/10.1016/0022-1694(93)90158-6).
- Dubey, S.K., Sharma, D., Babel, M.S., Mundetia, N., 2020. Application of hydrological model for assessment of water security using multi-model ensemble of CORDEX-South Asia experiments in a semi-arid river basin of India. *Ecol. Eng.* 143, 105641. <https://doi.org/10.1016/j.ecoeng.2019.105641>.
- Dudley, R.W., Hodgkins, G.A., McHale, M.R., Kolian, M.J., Renard, B., 2017. Trends in snowmelt-related streamflow timing in the conterminous United States. *J. Hydrol.* 547, 208–221.
- Estilow, T.W., Young, A.H., Robinson, D., 2015. A.: A long-term Northern Hemisphere snow cover extent data record for climate studies and monitoring. *Earth Syst. Sci. Data* 7, 137–142. <https://doi.org/10.5194/essd-7-137-2015>.

- FAO, 2022. FAOLEX Database: Pakistan, 11th Five Year Plan (2013-2018), retrieved on September 8, 2022 from <https://www.fao.org/faolex/results/details/en/c/LEX-FAOC202358/>.
- Evan, A., Eisenman, I., 2021. A mechanism for regional variations in snowpack melt under rising temperature. *Nat. Clim. Chang.* 11 (4), 326–330.
- Giorgi, F., Gutowski, W.J., 2015. Regional dynamical downscaling and the CORDEX initiative. *Annu. Rev. Env. Resour.* 40, 467–490. <https://doi.org/10.1146/annurev-enviro-102014-021217>.
- Gordon, B.L., Brooks, P.D., Krogh, S.A., Boisrime, G.F.S., Carroll, R.W.H., McNamara, J. P., Harpold, A.A., 2022. Why does snowmelt-driven streamflow response to warming vary? A data-driven review and predictive framework. *Environ. Res. Lett.* 17, 053004 <https://doi.org/10.1088/1748-9326/ac64b4>.
- Gutowski Jr., W. J., Giorgi, F., Timbal, B., Frigon, A., Jacob, D., Kang, H.-S., Raghavan, K., Lee, B., Lennard, C., Nikulin, G., O'Rourke, E., Rixen, M., Solman, S., Stephenson, T., Tangang, F. 2016. WCRP COordinated Regional Downscaling EXperiment (CORDEX): a diagnostic MIP for CMIP6, *Geosci. Model Dev.*, 9, 4087–4095.
- Harris, I., Osborn, T.J., Jones, P., Lister, D., 2020. Version 4 of the CRU TS monthly high-resolution gridded multivariate climate dataset. *Sci. Data* 7, 1–18.
- Hasson, S., 2016. Future water availability from Hindukush-Karakoram-Himalaya Upper Indus Basin under conflicting climate change scenarios. *Climate* 4, 40.
- Hersbach, H., Bell, B., Berrisford, P., Hirahara, S., Horányi, A., Muñoz-Sabater, J., Nicolas, J., Peubey, C., Radu, R., Schepers, D., Simmons, A., 2020. The ERA5 global reanalysis. *Q. J. R. Meteorol. Soc.* 146 (730), 1999–2049.
- Ho, C.K., Stephenson, D.B., Collins, M., Ferro, C.A., Brown, S.J., 2012. Calibration strategies: a source of additional uncertainty in climate change projections. *Bull. Am. Meteorol. Soc.* 93 (1), 21–26.
- Hodgkins, G.A., Dudley, R.W., Huntington, T.G., 2003. Changes in the timing of high river flows in New England over the 20th century. *J. Hydrol.* 278, 244–252. [https://doi.org/10.1016/S0022-1694\(03\)00155-0](https://doi.org/10.1016/S0022-1694(03)00155-0).
- Huss, M., Hock, R., 2018. Global-scale hydrological response to future glacier mass loss. *Nat. Clim. Chang.* 8 (2), 135–140.
- Immerzeel, W.W., Van Beek, L.P., Bierkens, M.F., 2010. Climate change will affect the Asian water towers. *Science* 328, 1382–1385.
- Hussain, M., Mahmud, I., 2019. pyMannKendall: a python package for non parametric Mann Kendall family of trend tests. *Journal of Open Source Software* 4 (39), 1556.
- Immerzeel, W.W., Lutz, A.F., Andrade, M., et al., 2020. Importance and vulnerability of the world's water towers. *Nature* 577, 364–369.
- Kam, J., Min, S.K., Kim, Y.H., Kim, B.H., Kug, J.S., 2022. Anthropogenic Contribution to the Record-Breaking Warm and Wet Winter 2019/20 over Northwest Russia. *Bull. Am. Meteorol. Soc.* 103 (3), S38–S43.
- Kam, J., Sheffield, J., 2016. Changes in the low flow regime over the eastern United States (1962–2011): variability, trends, and attributions. *Clim. Change* 135, 639–653. <https://doi.org/10.1007/s10584-015-1574-0>.
- Kam, J., Knutson, T.R., Milly, P.C., 2018. Climate model assessment of changes in winter-spring Streamflow timing over North America. *J. Clim.* 31, 5581–5593.
- Kang, D.H., Gao, H., Shi, X., ul Islam, S., Déry, S.J., 2016. Impacts of a rapidly declining mountain snowpack on streamflow timing in Canada's Fraser River basin. *Sci. Rep.* 6, 19299. <https://doi.org/10.1038/srep19299>.
- Kapnick, S.B., Delworth, T.L., Ashfaq, M., Malyshev, S., Milly, P.C.D., 2014. Snowfall less sensitive to warming in Karakoram than in Himalayas due to a unique seasonal cycle. *Nat. Geosci.* 7, 834–840. <https://doi.org/10.1038/ngeo2269>.
- Kehrwald, N.M., Thompson, L.G., Tandong, Y., Mosley-Thompson, E., Schotterer, U., Alfimov, V., Beer, J., Eikenberg, J., Davis, M.E., 2008. Mass loss on Himalayan glacier endangers water resources. *Geophys. Res. Lett.* 35.
- Kendall, M.G., 1975. Rank Correlation Methods. Griffin, London.
- Khan, A.J., Koch, M., Tahir, A.A., 2020. Impacts of climate change on the water availability, seasonality and extremes in the upper Indus Basin (UIB). *Sustainability* 12, 1283.
- Kim, J.-S., Kug, J.-S., Jeong, S.-J., Park, H., Schaepman-Strub, G., 2020. Extensive fires in southeastern Siberian permafrost linked to preceding Arctic Oscillation. *Sci. Adv.* 6, eaax3308. <https://doi.org/10.1126/sciadv.aax3308>.
- Knoben, W.J., Freer, J.E., Woods, R.A., 2019. Inherent benchmark or not? Comparing Nash-Sutcliffe and Kling-Gupta efficiency scores. *Hydrol. Earth Syst. Sci.* 23 (10), 4323–4331.
- Kumar, S., Merwade, V., Kam, J., Thurner, K., 2009. Streamflow trends in Indiana: Effects of long-term persistence, precipitation and subsurface drains. *J. Hydrol.* 374, 171–183. <https://doi.org/10.1016/j.jhydrol.2009.06.012>.
- Lettenmaier, D.P., Wood, E.F., Wallis, J.R., 1994. Hydro-climatological trends in the continental United States, 1948–88. *J. Clim.* 7, 586–607.
- Littlewood, I.G., Jakeman, A.J., 1994. A new method of rainfall-runoff modelling and its applications in catchment hydrology. *Comput. Mech. Publ.*
- Liu, Q., Piao, S., Janssens, I.A., Fu, Y., Peng, S., Lian, X.U., Ciais, P., Myneni, R.B., Peñuelas, J., Wang, T., 2018. Extension of the growing season increases vegetation exposure to frost. *Nature communications* 9 (1), 1–8.
- Lohmann, D., Nolte-Holube, R., Raschke, E., 1996. A large-scale horizontal routing model to be coupled to land surface parametrization schemes. *Tellus A* 48, 708–721. <https://doi.org/10.1034/j.1600-0870.1996.t01-3-00009.x>.
- Lohmann, D., Raschke, E., Nijssen, B., Lettenmaier, D.P., 1998. Regional scale hydrology: I. Formulation of the VIC-2L model coupled to a routing model. *Hydrol. Sci. J.* 43, 131–141. <https://doi.org/10.1080/02626669809492107>.
- Mann, H.B., 1945. Non-parametric tests against trend. *Econometrica* 13, 245–259.
- Mazhar, N., Mirza, A.I., Butt, Z.S., Butt, I.A., 2016. Monitoring decadal precipitation variability in Upper Indus Basin, Pakistan. *Pak. J. Sci.* 68, 352.
- Menzel, A., Fabian, P., 1999. Growing season extended in Europe. *Nature* 397, 659.
- Meresa, H., Zhang, Y., Tian, J., Faiz, M.A., 2022. Disentangling aggregated uncertainty sources in peak flow projections under different climate scenarios. *J. Hydrol.* 613, 128426.
- Mishra, V., 2015. Climatic uncertainty in Himalayan water towers. *J. Geophys. Res. Atmos.* 120, 2689–2705.
- Pakistan, F., 2009. Agriculture Project Report To USAID. *March*. <https://ipad.fas.usda.gov/pdfs/Pakistan/PakistanDecember2009MonthlyReport.pdf>.
- Nijssen, B., Lettenmaier, D.P., Liang, X., Wetzel, S.W., Wood, E.F., 1997. Streamflow simulation for continental-scale river basins. *Water Resour Res* 33 (4), 711–724.
- Ougahi, J.H., Cutler, M.E., Cook, S.J., 2022. Modelling climate change impact on water resources of the Upper Indus Basin. *Journal of Water and Climate Change* 13 (2), 482–504.
- Qin, Y., Abatzoglou, J.T., Siebert, S., Huning, L.S., AghaKouchak, A., Mankin, J.S., Hong, C., Tong, D., Davis, S.J., Mueller, N.D., 2020. Agricultural risks from changing snowmelt. *Nat. Clim. Chang.* 10, 459–465. <https://doi.org/10.1038/s41558-020-0746-8>.
- Rai, P., Choudhary, A., Dimri, A.P., 2019. Future precipitation extremes over India from the CORDEX-South Asia experiments. 137, 2961–2975. <https://doi.org/10.1007/s00704-019-02784-1>.
- Raju, P.V.S., Bhatla, R., Almazroui, M., Assiri, M., 2015. Performance of convection schemes on the simulation of summer monsoon features over the South Asia CORDEX domain using RegCM-4.3. *Int. J. Climatol.* 35, 4695–4706. <https://doi.org/10.1002/joc.4317>.
- Saeed, S., Müller, W.A., Hagemann, S., Jacob, D., 2011. Circum global wave train and the summer monsoon over northwestern India and Pakistan: the explicit role of the surface heat low. 37, 1045–1060. <https://doi.org/10.1007/s00382-010-0888-x>.
- Rehman, A., Jingdong, L., Du, Y., Khatoun, R., Wagan, S.A., Nisar, S.K., 2016. Flood disaster in Pakistan and its impact on agriculture growth (a review). *Environ. Dev. Econ* 6 (23), 39–42.
- Sakai, A., Fujita, K., 2017. Contrasting glacier responses to recent climate change in high-mountain Asia. *Scientific reports* 7 (1), 1–8.
- Sanjay, J., Krishnan, R., Shrestha, A.B., Raj Bhandari, R., Ren, G.Y., 2017. Downscaled climate change projections for the Hindu Kush Himalayan region using CORDEX South Asia regional climate models. *Adv. Clim. Chang. Res.* 8 (3), 185–198.
- Schwartz, M.D., Reiter, B.E., 2000. Changes in North American spring. *Int. J. Climatol.* 20, 929–932.
- Shahid, M., Rahman, K.U., 2021. Identifying the annual and seasonal trends of hydrological and climatic variables in the Indus Basin Pakistan. *Asia-Pac. J. Atmos. Sci.* 57, 191–205.
- Sheffield, J., et al., 2013. A drought monitoring and forecasting system for Sub-Saharan African water resources and food security. *Bull. Am. Meteorol. Soc.*, 95, 861–882, doi:10.1175/BAMS-D-12-00124.1. <https://doi.org/10.1175/BAMS-D-12-00124.1>.
- Sharif, M., Archer, D.R., Fowler, H.J., Forsythe, N., 2013. Trends in timing and magnitude of flow in the Upper Indus Basin. *Hydrol. Earth Syst. Sci.* 17 (4), 1503–1516.
- Siddiqui, R., Samad, G., Nasir, M., Jalil, H.H., 2012. The impact of climate change on major agricultural crops: evidence from Punjab, Pakistan. *Pak. Develop. Rev.* 51 (4), 261–276.
- Soncini, A., Bocchiola, D., Confortola, G., Bianchi, A., Rosso, R., Mayer, C., Lambrecht, A., Palazzi, E., Smiraglia, C., Diolaiuti, G., 2015. Future hydrological regimes in the Upper Indus Basin: A case study from a high-altitude glacierized catchment. *J. Hydrometeorol.* 16, 306–326. <https://doi.org/10.1175/JHM-D-14-0043.1>.
- Suman, M., Maity, R., 2020. Southward shift of precipitation extremes over south Asia: Evidence from CORDEX data. *Sci. Rep.* 10, 6452. <https://doi.org/10.1038/s41598-020-63571-x>.
- Usman, M., 2016. Contribution of agriculture sector in the GDP growth rate of Pakistan. *J. Glob. Econ.* 4, 1000184. <https://doi.org/10.4172/2375-4389.1000184>.
- Wasko, C., Nathan, R., Peel, M.C., 2020. Trends in global flood and streamflow timing based on local water year. *Water Resour Res* 56 (8), e2020WR027233.
- Yuan, X., Roundy, J.K., Wood, E.F., Sheffield, J., 2015. Seasonal forecasting of global hydrologic extremes: system development and evaluation over GEWEX basins. *Bull. Am. Meteorol. Soc.* 96, 1895–1912. <https://doi.org/10.1175/BAMS-D-14-00003.1>.
- Yaseen, M., Ahmad, I., Guo, J., Azam, M.I., Latif, Y., 2020. Spatiotemporal variability in the hydrometeorological time-series over Upper Indus River Basin of Pakistan. *Advances in Meteorology* 2020.